Available online at www.sciencedirect.com

ScienceDirect

Energy Procedia 92 (2016) 412 – 418

Energy Procedia

6th International Conference on Silicon Photovoltaics, SiliconPV 2016

Recombination behavior of photolithography-free back junction back contact solar cells with carrier-selective polysilicon on oxide junctions for both polarities

Michael Rienäcker[a,b,*], Agnes Merkle[a], Udo Römer[a], Heike Kohlenberg[a,b], Jan Krügener[b,c], Rolf Brendel[a,d], Robby Peibst[a,c]

[a]*Institute for Solar Energy Research Hamelin (ISFH), Am Ohrberg 1, D-31860 Emmerthal, Germany*
[b]*Laboratory of Nano and Quantum Engineering (LNQE), Leibniz Universität Hannover, Schneiderberg 39, D-30167 Hannover, Germany*
[c]*Institute of Electronic Materials and Devices, Leibniz Universität Hannover, Schneiderberg 32, D-30167 Hannover, Germany*
[d]*Institute of Solid State Physics, Leibniz Universität Hannover, Appelstr. 2, D-30167 Hannover, Germany*

Abstract

We report on ion-implanted, inkjet patterned back junction back contact silicon solar cells with **POL**ysilicon on **O**xide (POLO) junctions for both polarities – n^+ doped BSF and p^+ doped emitter. The recombination behavior is investigated at two different processing stages: before and after trench separation of p^+ and n^+ regions within polysilicon (poly-Si). Before trench separation, we find a systematic dependence of the recombination behavior on the BSF index, i.e. the p^+n^+-junction meander length in the poly-Si. Obviously, recombination at the p^+n^+-junction in the poly-Si limits the implied open circuit voltage $V_{oc,impl.}$ at one sun illumination and the implied pseudo fill factor $pFF_{impl.}$ to 695 mV and 80 %, respectively. After trench isolation, however, $V_{oc,impl}$ ($pFF_{impl.}$) values increase up to 730 mV (85.5 %), corresponding to a pseudo-efficiency of 26.2 % for an assumed short circuit current density J_{sc} of 42 mA/cm^2. We demonstrate a photolithography-free back junction back contacted solar cell with *p*-type and *n*-type POLO junctions with an in-house measured champion efficiency of 23.9 % on a designated area of 3.97 cm^2. This efficiency is mainly limited by the imperfect passivation in the undoped trench regions and at the undoped front side.

Peer review by the scientific conference committee of SiliconPV 2016 under responsibility of PSE AG.

*Keywords:*back junction back contact solar cell; polysilicon on oxide junctions; POLO; *pn* junction; trench isolation; recombination

* Corresponding author. Tel.: +49-5151-999-634;
E-mail address: m.rienaecker@isfh.de

Peer review by the scientific conference committee of SiliconPV 2016 under responsibility of PSE AG.
doi:10.1016/j.egypro.2016.07.121

1. Introduction

In recent years many research groups have investigated different types of carrier-selective junctions for high efficiency silicon solar cells [1]. The back junction back contact (BJBC) cell with hydrogenated amorphous silicon (*a*-Si:H)/ monocrystalline silicon (*c*-Si) heterojunctions, reaching an energy conversion efficiency of 25.6 % [2], is an excellent and well-known example for carrier-selective junctions, which were integrated into high efficiency silicon solar cells. A drawback of the *a*-Si/*c*-Si heterojunction technology for the application in BJBC cells is the restriction to low temperature processing and therefore a rather complex pattering procedure for the formation of interdigitated junctions and metallization on the rear side [3]. Shadow masked ion implantation is an enabling local doping technique for the junction formation on the rear side of BJBC cells to reduce the process complexity [4-8]. Nevertheless thermal stability of the junctions is required therefor.

In the late 1970s and early 1980s different groups proposed polysilicon emitters with an interfacial oxide as carrier-selective junctions for silicon solar cells with high temperature stability [9-13]. This type of junctions are denoted as **POL**ysilicon on **O**xide (POLO) junctions in the following [14-16]. Excellent results have recently been achieved with these junctions. In particular, saturation current densities as low as for *a*-Si/*c*-Si junctions, but lower junction resistivities for both electron collecting junctions based on n^+ POLO and hole collecting junctions based on p^+ POLO have been achieved [1,15,17-22]. This comparison between *a*-Si/*c*-Si heterojunctions and our temperature stable POLO junctions implies an efficiency potential larger than 25 % for both approaches and a potentially reduced process complexity for the latter [8].

So far, many groups [17-21] have reported promising implied open circuit voltages and pseudo fill factors for test structures and BJBC cell precursors with POLO junctions for both polarities. Yang *et al.* just recently published first photolithography patterned POLO-BJBC solar cells with an efficiency of 19.2 % [21].

One key challenge for the integration of these junctions into BJBC cells is the poor recombination behavior of *pn*-junctions formed within highly defective poly-Si [23, 20]. We therefore investigate the influence of a trench, separating p^+ and n^+ regions within poly-Si, on the recombination behavior on cells. We show promising results for BJBC solar cells with POLO junctions for both polarities with an in-house measured efficiency of 23.9 % (designated area of 3.97 cm^2). As patterning technique, we use inkjet-printed masks (which eventually can be substituted by screen printed masks) in combination with wet chemical etching. Although local doping is envisaged to be eventually performed via masked ion implantation, we also use inkjet printing for patterning of dielectric implant masks here to mimic masked ion implantation, but with a more flexible mask for the evaluation of different cell geometries.

2. Experimental

We use saw-damage etched 156 mm × 156 mm *n*-type Czochralski silicon wafers with a base resistivity of 3.5 Ωcm and a thickness of 160 µm as substrate material. In order to blind out resistive losses in the metallization as well as busbar losses in a first step, 20 small cells with an active cell area of 20 mm × 20 mm are processed on each wafer. In addition, full-area implanted boron and counterdoped (boron overcompensated by phosphorus) reference regions are integrated on the wafer to facilitate process monitoring.

After growing a ~2.1 nm thin thermal silicon dioxide layer in a tube furnace, undoped amorphous silicon (*a*-Si) is deposited on both sides by using low pressure chemical vapor deposition (LPCVD). Hereafter the front (rear) side of the wafer receives a blanket phosphorus (boron) implantation, followed by a masked phosphorus implantation on the rear.

The latter locally overcompensates the boron in an interdigitated pattern with different BSF indices ranging from 730 µm to 1175 µm (Fig. 1a). For masking of the phosphorus implantation, we pattern a sputtered dielectric layer by inkjet-printed hotmelt wax and a subsequent wet-chemical etching.

After removal of the dielectric implant mask, high temperature treatment for the formation of the POLO junctions (dopant activation, crystallization of the *a*-Si, and perhaps local break-up of the interfacial oxide) is performed. During this step, a thick silicon dioxide layer is grown on top of the poly-Si by wet thermal oxidation. Subsequently, this silicon dioxide layer is again patterned via inkjet printing on the rear, and removed from the front side of the wafer. The remaining SiO_2 on the rear acts as etching barrier for a subsequent texturization process, which yields a

textured front side and a separation of n^+ POLO BSF and p^+ POLO emitter regions by a textured trench. After removing the SiO_2 mask, the cell precursors are passivated with silicon nitride double layers on both sides and a silicon dioxide layer is deposited on the rear side. Via openings in the rear side dielectric layers are created by using inkjet patterning and wet chemical etching, whereas the front side passivation is removed during this step. After that, the front side is passivated again with a silicon nitride double layer and a silicon dioxide layer is deposited on the front side in order to improve its optical properties. An aluminium metallization of the rear side by vacuum evaporation in an industrial high-throughput tool from Applied Materials, followed by a self-aligned RISE contact separation [24,25] completes the cell process.

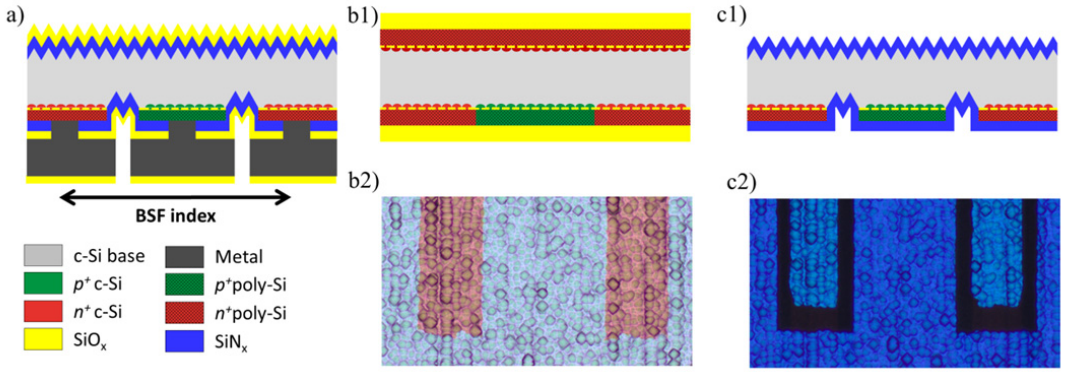

Fig.1. (a) Schematic drawing of a BJBC cell with POLO junctions for both polarities, (b1) cell precursor before and (c1) after texturization yielding a trench between the p^+ and n^+ poly-Si regions. (b2) and (c2) show the corresponding top view micrographs (field of view: 1200 µm × 600 µm) of the rear side of the cell precursors (b1, c1).

The recombination behavior of the solar cell precursors and reference test structures is characterized by injection dependent dynamic infrared lifetime measurements [26] before (Fig. 1b) and after (Fig. 1c) the trench isolation of the p^+ POLO emitter and the n^+ POLO BSF and after a subsequent via contact opening, metallization and RISE contact separation (final solar cells, Fig. 1a). After interpolation of the data points by cubic splines, $V_{oc,impl.}$ and $pFF_{impl.}$ values are extracted by assuming a J_{sc} value of 42 mA/cm^2. Recombination parameters $J_{0c,n+POLO}$ and $J_{0c,p+POLO}$ are extracted from photoconductance decay measurements on symmetric reference test structures according to the method of Kane and Swanson [27] and by using the Auger recombination model by Richter *et al.*[28]. A low resistance of the POLO junctions is verified by four point probe measurements in the reference regions according to Ref. [23] (ρ_{rel}~0.04) as well as on TLM test structures [22]. Solar cells are characterized with the solar cell analysis system LOANA from pvtools.

3. Results and discussion

Figures 2a and 2b show the arithmetic averages of injection dependent effective carrier lifetimes of cell precursors with five different BSF indices. Each average value is calculated using the measurement data for four cell precursors with the same BSF index on the same wafer.

While the high lifetimes measured in the reference regions demonstrate the excellent passivation quality of both the phosphorus ($J_{0c,n+ POLO}$ = 4 fA/cm²) and boron ($J_{0c,p+ POLO}$ = 7.5 fA/cm²) implanted poly-Si layers, the cell precursors exhibit remarkably poor recombination characteristics before trench isolation. As shown in Fig. 1b1), the BSF (n^+ POLO) and emitter (p^+ POLO) regions are in direct contact at this stage, i.e., a *pn*-junction is formed in the poly-Si. Due to the high defect density in the poly-Si, this *pn*-junction possibly has poor recombination behavior [18]. This picture is supported by the dependency of the lifetime level in Fig. 2a on the BSF index. For lower BSF indices, and therefore higher *pn*-junction meander length per cell area D_{pn}, the lifetime is reduced.

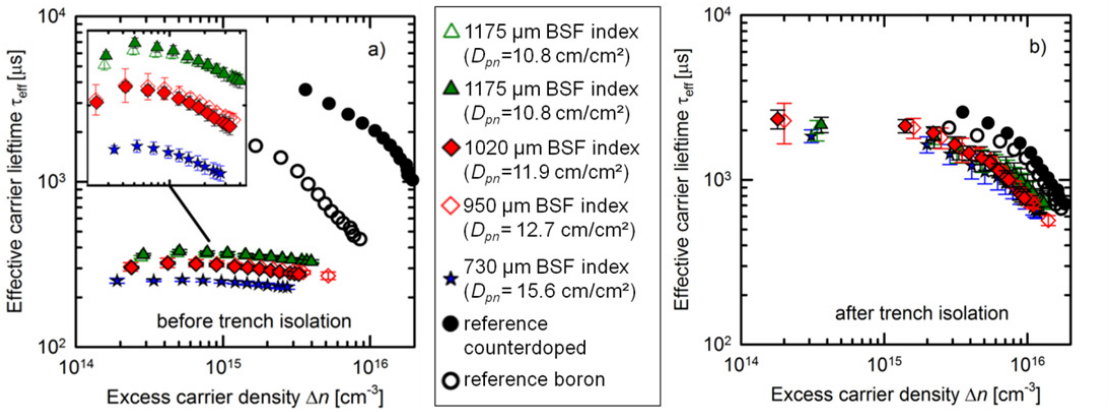

Fig.2. Average values (four cells) of injection dependent effective carrier lifetimes of cell precursors before (a) and after (b) trench isolation. Inset in Fig. 2 (a) is a magnification (effective carrier lifetime: 220 – 400 µs, excess carrier density: $2 \cdot 10^{14}$ – $4.5 \cdot 10^{15}$ cm^{-3}) of the lifetime curves of the cell precursors with different BSF indices, i.e. different p^+n^+-junction meander length densities D_{pn}.

Furthermore, the dependence of the effective lifetimes τ_{eff} on the injection level Δn shows a slight decrease of τ_{eff} for decreasing Δn. This behavior may be induced by a recombination path with an inherently high ideality factor (e.g. recombination within a space charge region). Alternatively, multiple recombination paths may be present, e.g. recombination at the p^+n^+-junction within poly-Si and at the poly-Si/c-Si interface. If the first exhibits an injection dependent transport limitation, a high effective ideality factor would be implied (equivalent circuit of a poor parallel diode connected via a resistor). However, further recombination paths might be present and contribute to the low lifetime level measured in the cell areas.

Measurements after the wet chemical removal of the *pn*-junction and passivation of the trench region (Fig. 1c1, c2) are shown in Fig. 2b. At this stage, the lifetime level and the overall recombination behavior of the cells is significantly improved: in low injection ~2 ms are measured for all BSF indices, which is comparable to the 2 ms (2.5 ms) of the full area boron (counterdoped) reference region. The slight decrease of the lifetimes in the reference regions is possibly caused by a reduced passivation quality of the SiN_x on the textured front side (compared to the previously planar front-side passivated with n^+ POLO).

The Figure 3a and 3b show the improvement of the implied open circuit voltage $V_{oc,impl.}$ at 1 sun illumination and of the implied pseudo fill factor $pFF_{impl.}$ due to the trench isolation for different BSF indices. For all investigated solar cell precursors, $V_{oc,impl.}$ values above 718 mV and $pFF_{impl.}$ values above 82.7 % are extracted, resulting in implied pseudo-efficiencies $\eta_{impl.}$ above 25 %. The highest implied pseudo-efficiency of 26.2 % is obtained on a cell precursor with an index of 1020 µm with an open circuit voltage $V_{oc,impl.}$ of 730 mV and a pseudo fill factor $pFF_{impl.}$ of 85.5 % (best cell precursor of four averaged cell precursors in Fig. 3).

After the trench isolation, we create via contact openings on the rear side, again by utilizing inkjet patterning and wet chemical etching. In this step, the front-side passivation, which was only deposited in order to facilitate lifetime measurements after the trench isolation, is removed. Therefore, the front-side was re-passivated with a SiN_x double layer stack. Eventually, we finalize the cell precursors by vacuum evaporation of aluminium on the rear side, followed by a self-aligned RISE contact separation. A strong and inhomogeneous degradation of $V_{OC,impl.}$ ($pFF_{impl.}$) between 9 mV (1.1 %) and 29 mV (4.6 %) is observed at this stage (Fig. 4). We attribute these losses to an increment of the recombination current density due to a poor re-passivation of the front side and/or a damage of the trench passivation on the rear side during the wet chemistry steps required for the opening of the contact vias. This hypothesis is supported by the fact that also the $pFF_{impl.}$ values are affected (Fig. 4b). In the framework of the two-diode model, this corresponds to an additional J_{02}-like recombination path at the undoped surfaces rather than to an increase of the J_{01}-like recombination at the heavily doped POLO junctions. This picture is furthermore confirmed by the implied *IV* characteristic.

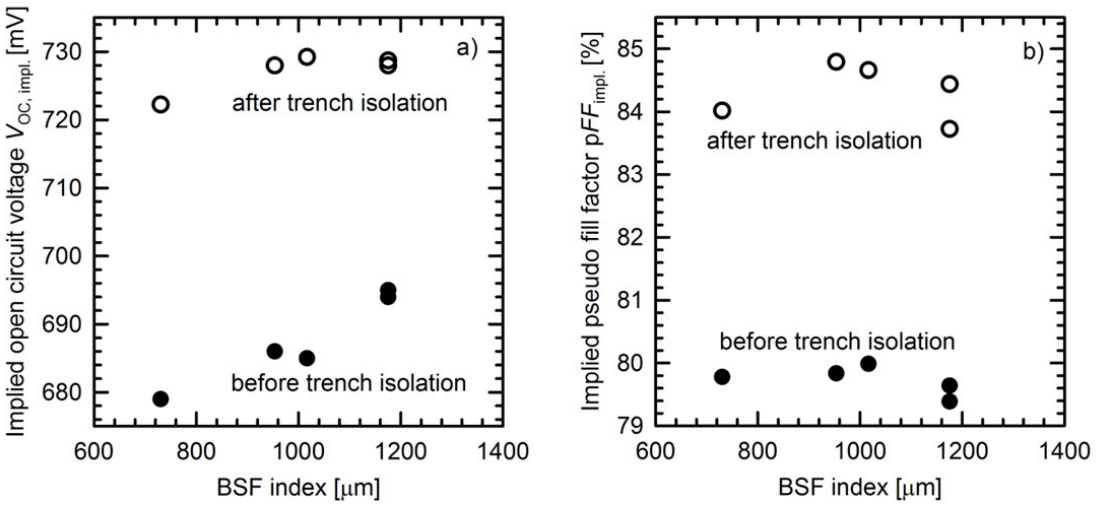

Fig.3. Comparison of the average values (four cells) of (a) implied open circuit voltage $V_{oc,impl.}$ and (b) implied pseudo fill factor $pFF_{impl.}$ (b) before and after trench isolation.

The best $V_{OC,impl.}$ and $pFF_{impl.}$ values we achieve on this wafer at this stage are 722 mV and 83.1 % for the solar cell with a BSF index of 1175 µm (best cell precursor of four averaged cell precursors in Fig. 4). We characterize this solar cell with the LOANA system and obtain an open circuit voltage V_{OC} of 720 mV and a pseudo fill factor *pFF* of 83.2 % resulting in a cell efficiency of 23.1 %.

This agreement between the extracted implied quantities and those extracted from *IV* data show that dynamic infrared lifetime measurements at different stages of cell process flow can be successfully used for process monitoring. The high open circuit voltages and pseudo fill factors after trench isolation demonstrates the potential of this cell concept to achieve high cell efficiencies.

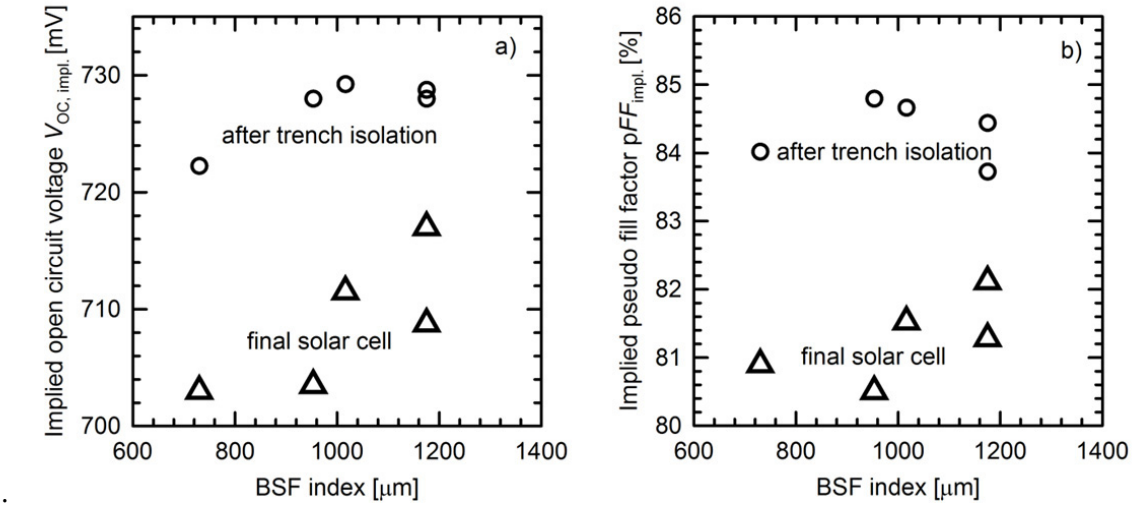

Fig.4. Comparison of average values (four cells) of (a) implied open circuit voltage $V_{oc,impl.}$ and (b) implied pseudo fill factor $pFF_{impl.}$ (b) after trench isolation and for final solar cells.

The champion efficiency of 23.9 % (in-house measurement on black chuck, designated area 3.97cm^2, V_{OC} 722 mV, J_{SC} 42.1 mA/cm², *FF* 78.7 %) is reached on a cell with a BSF index of 950 µm on a second wafer with a lower thermal budget during junction formation and by using an Al_2O_3/SiO_2 instead of SiN_x/SiO_2 rear side passivation. This efficiency is again mainly limited by the passivation of the undoped trenches, leading to low *pFF* of 81.2 %.

4. Conclusion

BJBC solar cells with carrier-selective **POL**ysilicon on **O**xide (POLO) junctions offer a promising high temperture route towards high efficiency silicon solar cells exceeding 25 %. Simulaneously, enabling techniques such as ion implantation can be applied to reduce process complexity. We have prepared photolithography-free ion-implanted BJBC solar cells with carrier-selective POLO junctions for both polarities based on inkjet patterning. The recombination behavior of two precursor stages - before and after trench isolation of p^+ and n^+ region within poly-Si - was compared. We found a clear correlation between p^+n^+-junction meander lenght density and injection dependent lifetimes. It was concluded that p^+n^+-junctions inside the highly defective poly-Si layer are responsible for the detrimental recombination behavior limiting the solar cell precursors $V_{OC,impl.}$ and $pFF_{impl.}$ to 695 mV and 80 %, respectively, when p^+ and n^+ regions within poly-Si are in contact.

Therefore p^+n^+-junctions in the poly-Si were removed by inkjet pattering of a thermally grown silicon dioxide layer and a subsequent alkaline texturization etch. This trench isolation strongly improved the recombination behavior of the solar cell precursors, enabling $V_{OC,impl.}$ ($pFF_{impl.}$) up to 730 mV (85.5 %) and a respective pseudo-efficiency of 26.2 %.

In this first cell run we achieved a champion efficiency of 23.9 % (in-house measurement on black chuck, designated area 3.97cm^2, V_{OC} = 722 mV, J_{SC} = 42.1 mA/cm², *FF*= 78.7 %). The good efficiencies achieved on final solar cells and the excellent implied *IV* characteristic determined on cell precursors show the high potential of this cell concept. We are confident to overcome the shortcomings of our first POLO-BJBC cell batch by optimizing the cell process and to realize conversion efficiencies beyond 24 %.

Acknowledgements

This work was performed in the framework of HERCULES. The project HERCULES has received funding from the European Union's Seventh Program for research, technological development and demonstration under grant agreement no. 608498.

The authors wish to thank Thomas Friedrich, Frank Heinemeyer, David Sylla and Nadine Wehmeier from ISFH for solar cells processing. We thank Guido Glowatzki and Bernd Koch from the Institute of Electronic Materials and Devices of Leibniz University Hanover for helping with ion implantation and the Laboratory of Nano and Quantum Engineering (LNQE) of Leibniz University of Hanover for support.

References

[1] A. Cuevas, T. Allen, J. Bullock, Yimao Wan, Di Yan and Xinyu Zhang, "Skin care for healthy silicon solar cells", in: *42nd IEEE Photovoltaic Specialist Conference (PVSC)*, 2015, pp. 1-6.

[2] K. Masuko, M. Shigematsu; T. Hashiguchi; D. Fujishima; M. Kai; N. Yoshimura; T. Yamaguchi; Y. Ichihashi; T. Mishima; N. Matsubara, T. Yamanishi; T. Takahama; M. Taguchi; E. Maruyama; S. Okamoto, "Achievement of More Than 25% Conversion Efficiency With Crystalline Silicon Heterojunction Solar Cell," in *IEEE Journal of Photovoltaics*, vol. 4, no. 6, pp. 1433-1435 (2014)

[3] J. Nakamura, N. Asano, T. Hieda, C.Okamoto, H. Katayama, and K. Nakamura, "Development of Heterojunction Back Contact Si Solar Cells", *IEEE Journal of Photovoltaic* vol. 4 no. 6, pp. 1491 – 1495, (2014)

[4] P. Sullivan, P. Nunan, and S. R. Walther, "Patterned assembly for manufacturing a solar cell and a method thereof", US Patent No. US 7820460, (2010)

[5] A. Grohe, R. Peibst, J. Graff, C. Schöllhorn, K. Meyer, Y. Larionova, U. Römer, T. Ohrdes, T. Wütherich, L. Bornschein, D. Stichtenoth, H.-J. Krokoszinski, N.-P.Harder, and P. Sullivan, "High-efficient ion implanted back contact cells for industrial application" in *27th EU PVSEC* (2012)

[6] C. B. Mo, S. J. Park, Y. J. Kim, D. Y. Lee, S. C. Park, D. S. Kim, S. B. Kim, J. Graff, M. Sheoran, and P. Sullivan, "High efficiency back contact solar cell via ion implantation", in *27th EU PVSEC* (2012)

[7] U. Römer, R. Peibst, T. Ohrdes, Y. Larionova, N.-P. Harder, R. Brendel, A. Grohe, D. Stichtenoth, T.Wütherich, C. Schollhorn, H.-J.Krokoszinski, J. Graff, "Counterdoping with patterned ion implantation", in *39th IEEE Photovoltaic Specialist Conference (PVSC)*, pp. 1280-1284, (2013)

[8] R. Peibst, U. Römer, Y. Larionova, H. Schulte-Huxel, T. Ohrdes, M. Häberle, B. Lim, J. Krügener, D. Stichtenoth, T. Wütherich, C. Schöllhorn, J. Graff and R. Brendel, "Building blocks for back-junction back-contacted cells and modules with ion-implanted poly-Si junctions", in *40th IEEE Photovoltaic Specialist Conference (PVSC)* (2014)

[9] J. Graul, A. Glasl and H. Murrmann, "High-performance transistors with arsenic-implanted polysil emitters," *IEEE Journal of Solid-State Circuits*, vol. 11, no. 4, pp. 491-495, (1976)

[10] T. Matsushita1, N. Oh-uchi, H. Hayashi and H. Yamoto, "A silicon heterojunction transistor", *Appl. Phys. Lett.* 35, 549, (1979)

[11] E. Yablonovitch, T. Gmitter, R. M. Swanson and Y. H. Kwark, "A 720 mV open circuit voltage SiO_x:c-Si:SiO_x double heterostructure solar cell", *Appl. Phys. Lett.* 47, 1211 (1985)

[12] F. Lindholm, A. Neugroschel, M. Arienzo, P. Iles, "Heavily doped polysilicon-contact solar cells", *IEEE Electron Device Letters* vol. 6, issue: 7, pp. 363 - 365 (1985)

[13] J. Y. Gan and R. M. Swanson, "Polysilicon emitters for silicon concentrator solar cells", in *22nd IEEE Photovoltaic Specialists Conference*, p. 245, (1990)

[14] R. Brendel, T. Dullweber, R. Gogolin, H. Hannebauer, N.-P. Harder, J. Hensen, S. Kajari-Schroeder, R. Peibst, J. H. Petermann, U. Römer, J. Schmidt, H. Schulte-Huxel, and V. Steckenreiter, in: Presentation of *28th EUPVSEC*, Paris, France, 2013

[15] R. Peibst, Y. Larionova, S. Reiter, M. Turcu, R. Brendel, D. Tetzlaff, J. Krügener, T. Wietler, U. Höhne and J.-D. Kähler, H. Mehlich, S. Frigge, submitted to *EUPVSEC2016*

[16] Peibst *et al.*,"Working principle of carrier selective poly-Si/c-Si juntions: Is tunneling the whole story?", *Solar Energy Materials and Solar Cells*, in preparation

[17] F. Feldmann, M. Bivour, C. Reichel, M. Hermle, S. Glunz, "Passivated rear contacts for high-efficiency n-type Si solar cells providing high interface passivation quality and excellent transport characteristics", *Solar Energy Materials and Solar Cells*, vol. 120, pp. 270-274 (2014)

[18] U. Römer *et al.*, "Ion Implantation for Poly-Si Passivated Back-Junction Back-Contacted Solar Cells", *IEEE Journal of Photovoltaics*, vol. 5, Issue: 2, pp 507-514 (2015)

[19] D. Yan, "Phosphorus-diffused Polysilicon Contacts for Solar Cells", *Solar Energy Materials and Solar Cells*, 2015

[20] D.L. Young *et al.*, "Interdigitated Back Passivated Contact (IBPC) Solar Cells Formed by Ion Implantation", *IEEE Journal of Photovoltaics*, Volume:PP, Issue: 99, Pages: 1-7 (2015)

[21] G. Yang, A. Ingenito, N. van Hameren, O. Isabella and M. Zeman, "Design and application of ion-implanted polySi passivating contacts for interdigitated back contact c-Si solar cells", *Appl. Phys. Lett.* 108, 033903 (2016)

[22] M. Rienäcker, Marcel Bossmeyer, Agnes Merkle, Udo Römer, Jan Krügener, Rolf Brendel, Robby Peibst, "Junction resistivity of carrier-selective polycrystalline / crystalline silicon junctions and its impact on the solar cell performance", submitted to *IEEE Photovoltaic Specialists Conference 2016*

[23] U. Römer, R. Peibst, T. Ohrdes, B. Lim, J. Krügener, E. Bugiel, T. Wietler, R. Brendel, "Recombination behavior and contact resistance of n^+ and p^+ poly-crystalline Si/ monocrystalline Si junctions", *Solar Energy Materials and Solar Cells*, Volume 131, Pages 85-91 (2014)

[24] P. Engelhart, N.P. Harder, T. Neubert, H. Plagwitz,B. Fischer, R. Meyer and R. Brendel, *Proceedings of the 21st EUPVSEC* pp. 773-776, (2006).

[25] A. Merkle, H. Schulte-Huxel, S. Blankemeyer, I.Feilhaber, R. Bock, V. Steckenreiter, S. Kajari-Schroeder,N.-P. Harder, R. Brendel, "From high-efficiency *n*-type solar cells to modules exceeding 20% efficiency with aluminum-based cell interconnection", *Progress in Photovoltaics* **21,** pp.1354-1362, (2013).

[26] K. Ramspeck, S. Reissenweber, J. Schmidt, K. Bothe, and R. Brendel, Appl. Phys. Lett. **93**, 102104 (2008)

[27] D. E. Kane and R. M. Swanson, "Measurement of the emitter saturation current by a contactless photoconductivity decay method," in *18th IEEE Photovoltaic Specialists Conference*, pp. 578–583, 1985

[28] A. Richter, S.W. Glunz, F.Werner, J. Schmidt, and A. Cuevas, "Improved quantitative description of Auger recombination in crystalline silicon", *Phys. Rev. B*, vol. 86, p. 165202, 2012